広島大学学位請求論文

Studies for controlling spin state by mixing metal and by mixing anion for the assembled Fe complexes bridged by bipyridine type ligands

ビピリジン型架橋配位子で架橋した集積型鉄錯体の金属混合と
アニオン混合によるスピン状態制御の研究

2016 年

広島大学院理学研究科
化学専攻

土手　遥

目次

1. 主論文

Studies for controlling spin state by mixing metal and by mixing anion for the assembled Fe complexes bridged by bipyridine type ligands

ビピリジン型架橋配位子で架橋した集積型鉄錯体の金属混合とアニオン混合によるスピン状態制御の研究

2. 公表論文

(1) Crystal structure and spin state of mixed crystals of iron with NCS and $NCBH_3$ for the assembled complexes bridged by 1,3-bis(4-pyridyl)propanes

H. Dote, H. Yasuhara, and S. Nakashima, *Journal of Radioanalytical and Nuclear Chemistry*, **2015**, 303, *2*, pp 1589-1593.

(2) Ligand Field of Fe(NCS)($NCBH_3$) Unit for the Assembled Complexes Bridged by 1,2-bis(4-pyridyl)ethane

H. Dote, M. Kaneko, K. Inoue, and S. Nakashima, in preparation.

(3) Formation Mechanism of Assembled Complexes Bridged by 1,3-bis(4-pyridyl)propane.

H. Dote, H. Yasuhara, and S. Nakashima, in preparation.

(4) Crystal structure and spin state of mixed-crystals of iron with zinc and cobalt for the assembled complexes bridged by 1,3-bis(4-pyridyl)propanes

H. Dote and S. Nakashima, *Hyperfine Interactions*, **2012**, 205, 1-3, 27-30.

(5) Spin state of mixed crystals of iron with zinc or cobalt for the assembled complexes bridged by 1,3- bis (4-pyridyl) propanes

S. Nakashima, H. Dote, M. Atsuchi, and K. Inoue, *J. Phys., Conf. Ser.*, **2010**, *217*, 012035

主論文

Contents

Chapter I
General Introduction

I. General Introduction

The design and synthesis of new molecule-based magnets are active areas in chemistry because the various magnetic properties are thought to be accessible through design. Self-assembled coordination polymers containing transition metal ions and organic bridging ligands have attracted intensive interests because of their potential abilities for selective inclusion and transformation of ions and molecules[1]. It is possible to construct various structures and have functions, for example, multifunctional solid-state properties including light- and pressure-induced magnetization[2], guest sensitivity[3], and electrical conduction have been reported[4]. Spin-crossover phenomenon (SCO) which is the change between high-spin state (HS) and low-spin state (LS) is an important factor for complex becoming memory device or switching materials.

I-1. Spin-crossover phenomenon (SCO) [5-8]

Transition metal complexes are surrounded by ligands and/or anions; therefore *d*-orbital is split. Transition metals having 4-7 *d*-electrons and octahedral structure can take HS or LS. For example, in the case of Fe(II), which has six *d*-electrons, S = 0 (LS) or S = 2 (HS) is observed, depending on ligand field strength.(Fig. I-1-1-1) When the ligand field strength is intermediate, the spin state changes depending on temperature, pressure, light irradiation. This is spin equilibrium or transition of spin state, which is called “spin-crossover phenomenon” (SCO). This phenomenon is induced by light, pressure, temperature, and so on. Thus the complexes have a possibility to become switching device for the bistability in attained.

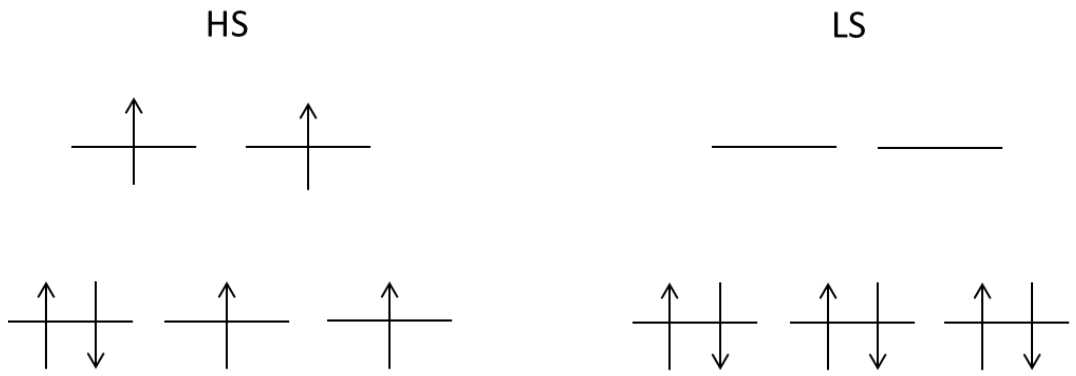

Fig. I-1-1 Spin state of HS and LS for Fe(II).

When complex is affected by temperature, the behaviour is classified by the shape of magnetic susceptibility curve as following;

I. Spin transition occurs with wide temperature region.

II. Spin transition occurs sharply.

III. Magnetic susceptibility curve has hysteresis loop.

IV. Magnetic susceptibility curve has stepwise transition.

V. Spin transition occurs incompletely.

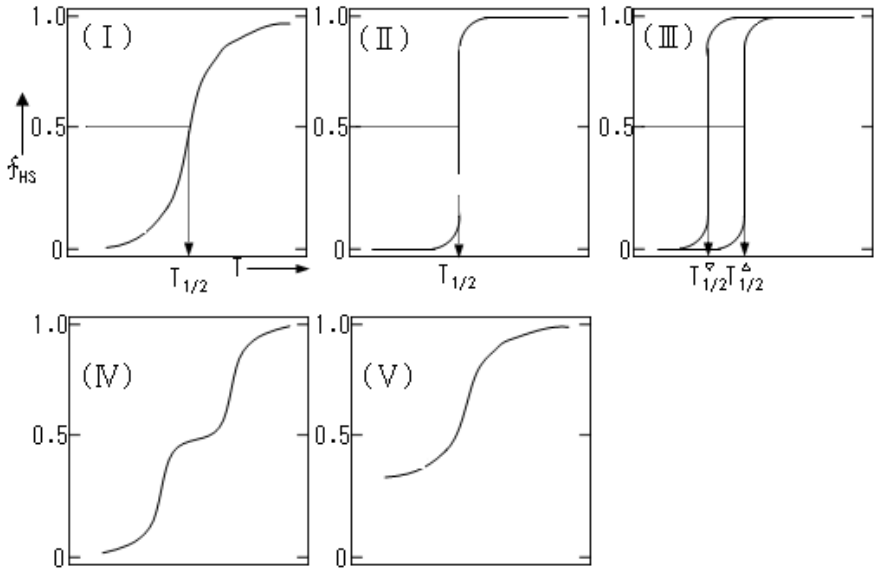

Fig. I-1-2 Spin transition for SCO complex.

I-2 SCO for assembled complexes

By assembling complexes, it is expected to show interaction among metals, and then the hysteresis loop might be observed around the SCO temperature. In 1995, J.A. Real, et al. synthesized assembled Fe^{II} complex bridged by 1,2-bis(4-pridyl)ethylene and the sample showed SCO[9]. While, in 2002, G. J. Halder, et al. showed guest-dependent SCO by using *trans*-4,4'-azopyridine[10]. As shown those literatures, SCO can be changed depending on whether guest molecules exist or not. Therefore we synthesized self-assembled complexes by using various bis(4-pyridyl) type ligands. We chose 1,2-bis(4-pyridyl)ethane (bpa) and 1,3-bis(4-pyridyl)propane (bpp) as bridging ligand, because a variety of assembled structure was expended depending on *anti- gauche*-conformer (Fig. I-2-1). In the clathration, $Fe(NCX)_2(bpa)_2 \cdot 2(p\text{-DCB})$ (X= S, Se: *p*-DCB= 1,4-dichlorobenzene) had shown SCO between HS and LS but complex having X = BH_3 can't clathrate *p*-DCB. However $Fe(NCBH_3)_2(bpa)_2 \cdot 2$(biphenyl) complex also showed SCO[11]. The spin transition temperature increases in order of X = S, Se, and BH_3. This tendency is based on ligand field strength.

The spin state of Fe^{II} complexes bridged by 1,3-bis(4-pyridyl)propane ligand was reported[12]. The complex has 2D interpenetrated structure without benzene molecules and 1D chain structure clathrating two benzene molecules per one iron. SCO occurs for complex with $NCBH_3$ without benzene while complexes clathrating benzene molecules do not show SCO phenomenon. SCO switching was observed accompanied by desorption and adsorption on benzene molecule.

Kaneko et al. revealed that SCO phenomenon is affected by dihedral angles of pyridyl-iron-pyridyl ligand[13]. $Fe(NCS)_2(bpp)_2 \cdot 2(p\text{-DCB})$ is parallel, $Fe(NCS)_2(bpa)_2$ is distorted propeller, and $Fe(NCBH_3)_2(bpa)_2$ is complete propeller. The two of the former are switching-off system whose metal does not show SCO phenomenon and the latter is switching-on system whose metal has SCO phenomenon.

So far, our group established to control the SCO-on or off. But it is not easy to control the transition temperature of SCO.

I-3 Aim of our study

To control the transition-temperature, we studied mixed complexes. To increase chemical pressure in the complexes, we performed mixed metal experiment with the metal having smaller radius. In addition, to control the ligand field, we also synthesized anion mixed complexes. The anion mixed complexes have NCS and $NCBH_3$ as anion ligand.

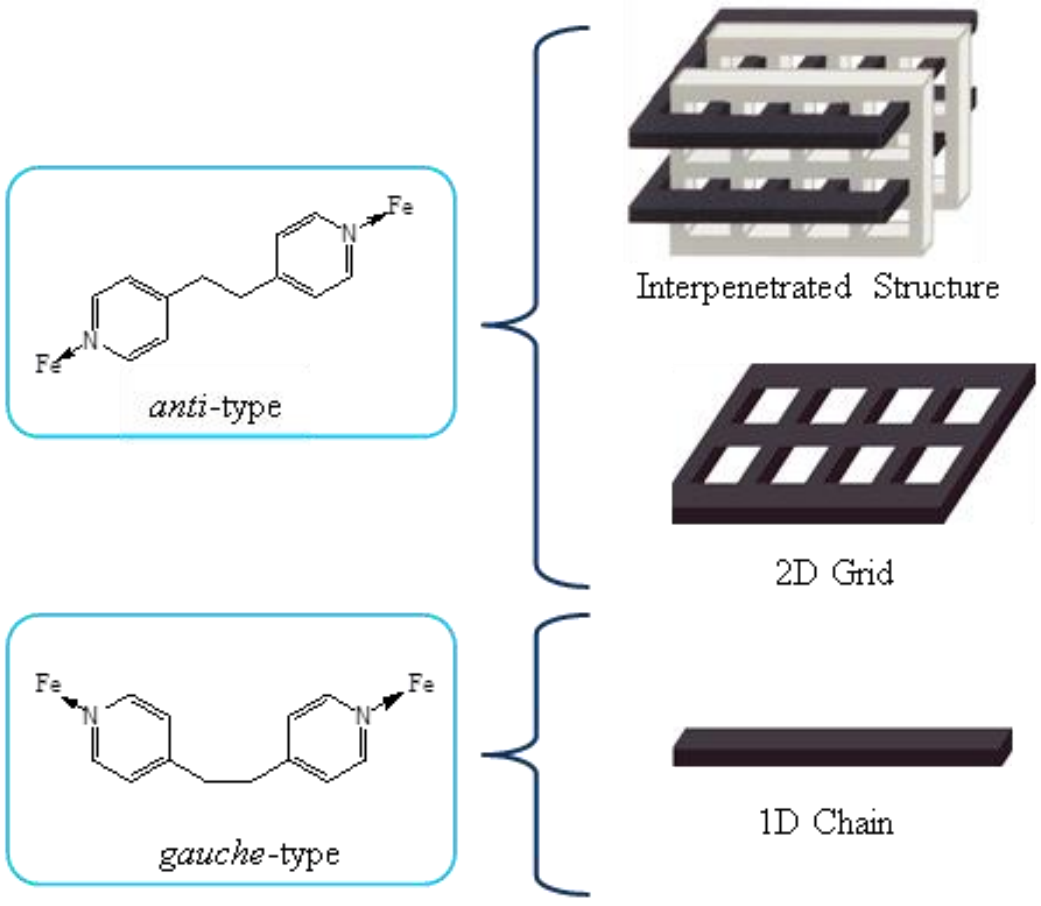

Fig. I-2-1 Various types of assembled structures of *anti*/*gauche* isomer by using bpa.

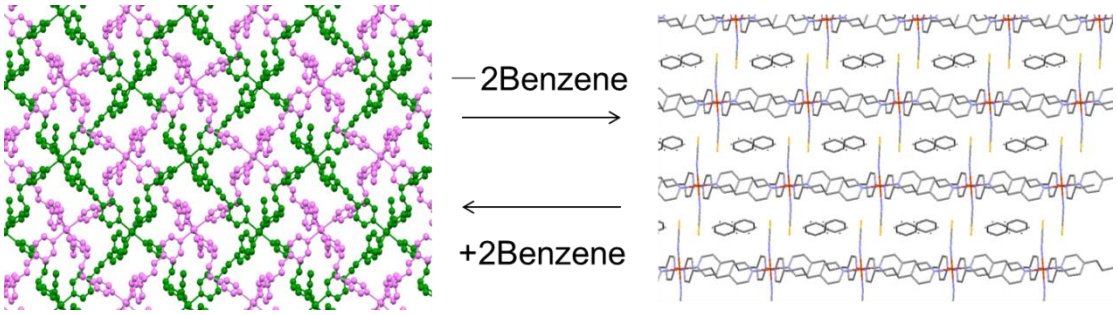

Fig. I-2-2 Structural switching of bpp complexes by using benzene molecules.

I-3 Reference

1. Moulton B, Zaworotko MJ, *Chem Rev,* **2001**, 101:1629
2. P. Gütlich, A. Hauser, H. Spiering, *Angew. Chem. Int. Ed.* **1994**, 33, 2024.
3. G. J. Halder, C. J. Kepert, B. Moubaraki, K. S. Murray, J. D. Cashion, *Science* **2002**, 298, 1762.
4. M. Kurmoo, A. W. Graham, P. Day, S. J. Coles, M. B. Hursthouse, J. L. Caulfield, J. Singleton, F. L. Pratt, W. Hayes, L. Ducasse, P. Guioneeau, *J. Am. Chem. Soc.* **1995**, 117, 12209.
5. S. Kitakawa, "Assembled metal complexes", *Kodansha Ltd*., Tokyo, **2006**
6. H. Okawa, T. Ito, "Chemistry of assembled complexes", *Kagaku-Dojin Ltd*., Kyoto, **2003**
7. M. Nishino, S. Miyashita, *The Physical Society of Japan,* **2002**, 57, 10, 728-737
8. K. Nakano, S. Kawata, K. Yoneda, A. Fuyuhiro, T. Yagi, S. Nasu, S. Morimoto, S. Kaizaki., *Chem. Commun*., **2004**, 2892-2893.
9. J. A. Real, E. Andrés, M. C. Muñoz, M. Julve, T. Granier, A. Bousseksou, F. Varret, *Science* **1995**, *268*, 265.
10. G. J. Halder, C. J. Kepert, B. Moubaraki, K. S. Murray, J. D. Cashion, *Science* **2002**, *298*, 1762.
11. T. Morita, S. Nakashima, K. Yamada, K. Inoue, *Chem. Lett*. **2006**, 35, 1042.
12. M. Atsuchi, H. Higashikawa, Y. Yoshida, S. Nakashima, and K. Inoue, *Chem. Lett.*, 2007, *36*, 1064.
13. M. Kaneko, and S. Nakashima., *Bull. Chem. Soc. Jpn., **2015**, 88, 8, 1164-1170*.

Chapter II

Theoretical Section

II. Mössbauer spectroscopy [1,2]

II-1. General outline of ^{57}Fe Mössbauer spectroscopy

Mössbauer spectroscopy is a useful method to know information about nucleus. The nucleus doesn't exist independently, but t interacts with surrounding electrons. That is to say, to get the information on nucleus means to get information on surrounding electrons, for example, oxidation number and spin state, etc. Absorption resonance is phenomenon which is obtained as absorption spectra by using natural light. We consider two atoms (or electrons) having same energy level and one is excited state, and the other is ground state. Excited state is unstable, so the atom releases energy and becomes ground state, and it is possible that the other atom accepts the energy and becomes excited state. ^{57}Fe nucleus is known as the most popular Mössbauer nucleus by reasons of lower resonance energy and a huge variety of iron compounds.

In Mössbauer spectroscopy, the energy scale is a unit of velocity because the difference of energy is given by the Doppler Effect from motion of γ-ray source. The alternation of Mössbauer γ-ray energy is expressed by

$$\Delta E = (v/c)E\gamma \qquad \cdots(1)$$

where ν is Doppler velocity, c is velocity of light and Eγ is γ-ray energy. Besides the environment of γ-ray source is as the same as that of absorber, an absorption peak exists only in the position of 0 velocities. However energy level of nuclear is affected by environment of surrounding negative charge. Therefore, to refer following Mössbauer hyperfine interactions make sense to know electronic state in the target atom.

The characteristic of Mössbauer spectroscopy is identifying the spin state of one metal. Magnetic susceptibility measurement shows spin state of average of all metals. While Mössbauer spectroscopy can distinguish one spin state and the others, and show different spectra depending on environment around metal.

II-2 Isomer shift (I.S.)

The isomer shift means a change in the electronic monopole (Coulombic) interaction between electronic and nuclear charges.

In many cases a nucleus is assumed as point charge for simplification. But the nucleus has a finite size and changes by excitation. An s-electron wave function has a finite value inside the nuclear radius.

When the nucleus is spherical with a radius R, and electron density at nuclear position is $|\Psi(0)|^2$, the interaction energy is expressed as

$$\mathrm{E} = {}^{2\pi}/_{5}\, Z\mathrm{e}^2|\Psi(0)|^2R^2 \qquad \cdots(2)$$

where Z is atomic number and e is electronic charge. When the electron density at nuclear position is different between γ-ray source and absorber, the shift is as

$$\Delta\mathrm{E} = {}^{2\pi}/_{5}\, Z\mathrm{e}^2\{|\Psi(0)|_A^2 - |\Psi(0)|_S^2\}R^2 \qquad \cdots(3)$$

where A and S in subscripts mean Absorber and Source, relatively. Moreover, the nuclear size is not constant but different between ground and excited states. Therefore,

$$\Delta\mathrm{E} = {}^{2\pi}/_{5}\, Z\mathrm{e}^2\{|\Psi(0)|_A^2 - |\Psi(0)|_S^2\}((R+\delta R)^2 - R^2) \quad \cdots(4)$$

where δR means variation of the nuclear radius and R means radius for ground state. In the case of ^{57}Fe nucleus, the nucleus reduces by 0.052 % in excitation. Since $R >> \delta R$ and δR is a characteristic value for each nucleus,

$$\delta = \Delta\mathrm{E} = \mathrm{C}\{|\Psi(0)|_A^2 - |\Psi(0)|_S^2\} \qquad \cdots(5)$$

where C (= ${}^{4\pi}/_{5}\, Z\mathrm{e}^2(R \cdot \delta R)$) is constant number for each nucleus and the energy difference ΔE is called as *isomer shift* (I.S.) designated by symbol δ.

It is shown that the I.S. depends on only difference between $|\Psi(0)|_A^2$ and $|\Psi(0)|_S^2$. In ions of the transition metals such as ^{57}Fe, the valence changes occur as the change in *d*- (or *f*-) electron numbers having no electron density at nucleus. Evidently, only *s*-electron orbital has electronic density at nucleus. However, *s*-electrons are affected by the shield from *d*- or *f*- electrons, as a result *s*-electron orbital expands and $|\Psi(0)|^2$

reduces. Therefore, the I.S. reflects *d*- or *f*- electron number, i.e. oxidation number. Ferrous ion shows larger I.S. than ferric ion generally because the constant C of ^{57}Fe is negative.

II-3 Quadrupole splitting value (Q.S.)

Quadrupole splitting value (Q.S.) means an electric quadrupole interaction between nuclear quadrupole moment and local electric field gradient tensor at the nucleus. This resembles NQR.

A nucleus having a nuclear spin $I > 1/2$ has an electric quadrupole moment, eQ, which is characteristic to each nucleus, and shows a quadrupole hyperfine splitting by interacting with electric field gradient. The nuclear quadrupole moment, Q, is the deviation from spherical symmetry of the nuclear charge and expressed by

$$eQ = \int \rho r^2 (3\cos^2\theta - 1) d\tau \quad \cdots(6)$$

where, +e is the charge on the proton and ρ is the charge density in the volume element dτ at a distance r from the center of the nucleus and at an angle θ to the axis of the nucleus spin.

The Hamiltonian for the interaction of the nuclear quadrupole moment with the electronic environment is expressed by

$$\mathrm{H} = {e^2qQ}\Big/{4I(2I-1)}\,[3I_z^2 - I(I+1) + \eta\left(I_x^2 - I_y^2\right)] \quad \cdots(7)$$

where $eq = V_{zz}$ is the electric field gradient (along the z-direction) and $\eta = (V_{xx}\text{-}V_{yy})/V_{zz}$ is the asymmetry parameter describing the difference in electric field gradient in the x and y directions, the directions are defined as $|V_{xx}| \leq |V_{yy}| \leq |V_{zz}|$. If $\eta = 0$ and $I = 3/2$, expression (7) is given by

$$\mathrm{E}_Q = {e^2qQ}\Big/{4I(2I-1)}\,[3I_z^2 - I(I+1)](1 + {\eta^2}/{3})^{1/2}] \quad \cdots(8)$$

with energy level at $\pm(^{e^2qQ}/_4)(1+{}^{\eta^2}/_3)^{1/2}$.

In the spin state of ^{57}Fe nucleus $I_g = 1/2$ and $I_e = 3/2$, the ground state with $I_z = \pm 1/2$ is not split and the excited state has two levels with $I_z = \pm 1/2$ and $\pm 3/2$ split by $(e^2qQ/2)(1+\eta^2/3)^{1/2}$. Therefore two absorption peaks appear in ^{57}Fe Mössbauer spectrum and a difference between their energies is corresponding to Q.S. designated by symbol ΔE_Q.

As $0 \leq \eta \leq 1$, the value of asymmetry term in the splitting value, $(e^2qQ/2)(1+\eta^2/3)^{1/2}$, takes from 1 to 1.15 and the influence on Q.S. is little and usually able to be ignored. Therefore eq defines the quadrupole splitting value and q is expressed by

$$q = q_{val}(1-R)+q_{lat}(1-\gamma_\infty) \quad \cdots(9)$$

where the first term is influence from valence electrons and second term is that on distorted inner electrons by ligand and/or anions. R and γ_∞ are called Sternheimer shielding factor and show degree of polarization. Although the effect of γ_∞ is large, the effect of second term is less than that of the first term, since electronic field gradient is in proportion to cube of distance. Therefore the distribution of valence electron is estimated by ΔE_Q, e.g. Fe(II) high-spin (HS, S = 2) and Fe(III) low-spin (LS, S = 5/2) have large ΔE_Q, and Fe(II) LS (S = 0) and Fe(III) HS (S = 1/2) have small ΔE_Q. However it should be remembered to be unable to ignore the second term and it is hard to decide apparently in some cases.

II-4. Spin-crossover phenomenon (SCO) [3-6]

As shown section-I, when complex is induced by temperature, the behaviour classifies shape of magnetic susceptibility curve as following;

I. Spin transition occurs on wide temperature region.

II. Spin transition occurs sharply.

III. Magnetic susceptibility curve have hysteresis loop.

IV. Magnetic susceptibility curve have stepwise transition.

V. Spin transition occurs incompletely.

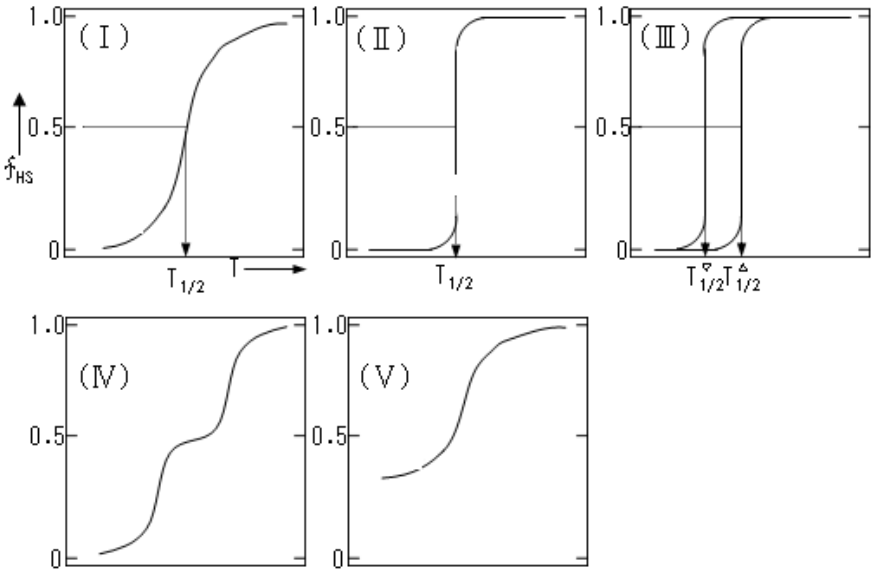

Fig. I-2-4-1 Spin transition for SCO complex.

For I-III, it results from strength of intermolecular interaction (hydrogen bonding or π-π stacking). There is analysis method, called "domain model", which estimates strength of intermolecular interaction from fraction of HS. In that theory, we presume size of system is N_A (Avogadro constant) and n molecules construct domains and change with each other. Amount of domains are $N=N_A/n$ and individual domain is completely HS or LS. In this case, Gibbs function of all system is

$$\mathbf{G}=f_{HS}\mathbf{G}_{HS}+(1-f_{HS})\mathbf{G}_{LS}+Nk_BT(f_{HS}\ln f_{HS}+(1-f_{HS})\ln(1-f_{HS})) \quad \cdots(10)$$

and fraction of HS in equilibrium is

$$f_{HS} = {}^{1}/_{1+\exp(\Delta \boldsymbol{G}/Nk_BT)} = {}^{1}/_{1+\exp(\Delta \boldsymbol{G}/RT)} \quad \cdots(11)$$

where N is amount of domains and $\Delta \boldsymbol{G}$ is difference of free energy between HS and LS (G_{HS}-G_{LS}). This equation transforms by using equilibrium constant into

$$\frac{d}{dT}\ln K = {n\Delta H}/{RT^2} \quad , \quad K = {f_{HS}}/{f_{LS}} = {f_{HS}}/{(1 - f_{HS})} \quad \cdots (12)$$

where ΔH is difference of Hamiltonian energy between HS only and LS only (H_{HS}-H_{LS}). If we can regard temperature on f_{HS}=1/2 as center of the transition (T_c) and ΔH as constant ($\Delta H(T)=\Delta H_{trs}$),

$$f_{HS} = {1}\Big/{1 + \left(\left[{n\Delta H_{trs}}/{R}\left({1}/{T} - {1}/{T_c}\right)\right]\right)}$$

that is change value of f_{HS} is characteristics by n. This n is considerable as parameter showing how cooperative molecule behaves. For example if complex has strong interaction and shows the transition II, n corresponds to ∞. In this case, the transition may have hysteresis loop and the loop often has temperature width from 5K to 10K.

SCO may show complex phase transition. The first example of transition IV is compound $[Fe(2\text{-pic})_3]Cl_2 \cdot EtOH$ (2-pic=2-picolylamine). The plateau of this middle step was researching over 20 years. In the present study, it is identified $[Fe(2\text{-pic})_3]^{2+}$ is infinite chain having HS and LS in turn[3].

Similar phenomenon can be occurred at binuclear complex, known as $[Fe(L)(NCX)_2]_2(bpym)$ (L=2,2'-bipyrimidine(bpym), 2,2'-bithiazoline(bt))(X=S,Se) and $[Fe(phdia)_2(NCS)_2]_2(phdia)$ (phdia=4,7-phenanthroline-5,6-diamine)[4]. In these cases, iron is [HS-LS] state in the plateau and spin transition is from [HS-HS] to [HS-LS] and from [HS-LS] to [LS-LS]. In other case, [HS-HS] and [LS-LS] pair exists in the plateau for $[Fe(NCBH_3)(4phpy)]_2(bphpy)_2$ (4phpy = 4-phenylpyridine) , (bphpy=3,5-bis(2-pyridyl)pyrazole)[5]. In general we cannot draw structure of binuclear pear of [HS-LS]. But nowadays we can analyse this state for $[Fe_2(PMAT)_2](BF_4)_4 \cdot DMF$ (PMAT=1,2,4-triazole-based acyclic ligand)[6].

Finally V is incomplete spin transition. This is the case that the sample usually has misalignment or defect, so a little residue of HS exists at low temperature.

II-5. Reference

1. T. C. Gibb, “Principles of Mössbauer spectroscopy”, *Champman and Hall Ltd*., London, **1976**
2. H. Sano, “Mössbauer spectroscopy –The Chemical Applications-“, *Kodansha Ltd*., Tokyo, **1972**
3. S. Kitakawa, “Assembled metal complexes”, *Kodansha Ltd*., Tokyo, **2006**
4. H. Okawa, T. Ito, “Chemistry of assembled complexes”, *Kagaku-Dojin Ltd*., Kyoto, **2003**
5. M. Nishino, S. Miyashita, *The Physical Society of Japan,* **2002**, 57, 10, 728-737
6. K. Nakano, S. Kawata, K. Yoneda, A. Fuyuhiro, T. Yagi, S. Nasu, S. Morimoto, S. Kaizaki., *Chem. Commun*., **2004**, 2892-2893.

Chapter III

Experimental Section

III-1 Elemental analysis

Elemental analysis for C, H, N, and S were performed on Perkin Elmer 2400II CHNS/0 Analyzer twice in each sample at the Natural Science Center for Basic Research and Development (N-BARD), Hiroshima University. To determine the fraction of NCS we fitted the data for experimental data and calculation data by changing the fraction of NCS by 0.05 and the fraction of *p*-DCB or benzene by 0.1 for *p*-DCB or benzene inclusion complexes, respectively.

III-2 Powder X-ray diffraction pattern

The powder X-ray diffraction patterns (PXRD) were measured on a Rigaku RAD-X system using Cu-Kα radiation and employing a scan rate of 5.0 °/min, step of 0.02 °, and region from 5.0 ° to 60.0 °. All measurements were performed under air at room temperature (RT).

III-3 Single crystal X-ray diffraction analysis

All diffraction data were collected by in-situ measurements using a Bruker SMART-APEX diffractometer equipped with CCD area detector and graphite-monochromated Mo-Kα radiation, λ=0.771073 Å, ω-scan mode (0.3 °-steps). Semi-emperical absorption corrections on Laue equivalents were applied. The structures were solved by direct methods and refined by full-matrix least-squares against F^2 of all data using SHELX-97. Hydrogen atoms on carbon atoms were included in calculated except for *p*-DCB enclathrated complex having 1D structure. For the complex, all atoms including hydrogens are determined. All the atoms except for hydrogens were refined anisotropically, but unfortunately EtOH molecules could not be determined for complex having interpenetrated structure with bpa.

III-4 Mössbauer spectroscopy

A ^{57}Co(Rh) source moving in constant-acceleration mode was used for ^{57}Fe Mössbauer spectroscopic measurements. Variable temperature ^{57}Fe Mössbauer spectra were obtained by using Tokyo Research spectrometer and a continuous-flow crystat or handmade high temperature apparatus. The Mössbauer parameters were obtained by least-squares fitting to Lorentzian peaks. The isomer shift values are referred to metallic iron.

III-5 ICP-OES analysis

ICP Optical Emission Spectrometer is performed by SPS3510 made in *SII Nano Technology Inc*. Scan sample liquid is processed that one crystal is sunk in ultrapure water and dissolved. If crystal can't be dissolved, crystal is crushed by using glass stick until crystal can't be seen. Calibration curves are drawn by measuring intensity of 1 ppm, 0.5 ppm, 0.1 ppm, and 0.01 ppm iron and zinc standard solution and 0.994 ppm, 0.497 ppm, 0.099 ppm, and 0.050 ppm cobalt standard solution and ultrapure water. Scan point of iron, zinc, and cobalt is 238.204 nm, 202.548 nm, and 228.616 nm, respectively.

III-6 UV-vis spectroscopy

UV spectra were measured using JASCO V-650DS spectrometer and attached ISV-722/723 60 mm Integrating Spheres from 900 nm to 300 nm and step of 0.5 nm.

III-7 Magnetic measurements

Magnetic measurements was carried out by using Quantum Design MPMS-5S SQUID measurement. Magnetic field being 1000 G, from 2 to 50 K by 2 K at a time, from 50 to 160 K by 1 K at a time, and from 160 to 300 K by 10 K at a time, or from 2 to 300 K by 2 K at a time for three times per one point, then decreased with the same speed.

III-8 DFT calculations

All the DFT calculations were performed by using the program "ORCA" package[1]. A mononuclear pyridine model in which bpa was replaced by pyridine, $[Fe(NCX)_2(py)_4]$ (X= S, Se, and BH_3; py: pyridine) was created by cutting out a single-crystal X-ray structure. Geometry optimization was performed at BP86/SV(P) level constraining the dihedral angle between Fe-NCX axis and pyridine plane. All self-consistent field calculations were carried out by TPSSh/TZVP method which reproduced the energy difference between HS and LS state for Fe^{II} SCO complexes.

III-9 Reference

1. Neese F, *WIREs Comput. Mol. Sci.*, **2012**, 2, 73-78

Chapter IV

Two metals mixed complexes

IV Summary of chapter IV

Mixed complexes enclathrating benzene molecules and manganese were synthesized. Powder X-ray diffraction pattern shows that complexes enclathrating benzene molecules are 2D interpenetrated structure and Mössbauer spectroscopy shows that all complexes have temperature-independent HS. In addition this, desorption benzene sample, which was kept in room temperature, shows SCO phenomenon for NCSe and $NCBH_3$ complex. This behavior also shows for pure iron complexes.

While manganese mixed complexes have similar characteristics to pure iron complexes. Notably difference is $NCBH_3$ complex for metal-mixed complex has more HS than pure iron complex. This depends on chemical pressure caused by diluted iron by manganese which has larger ionic radius.

Chapter V

Three metals-mixed complexes[1]

[1] Formation Mechanism of Assembled Complexes Bridged by 1,3-bis(4-pyridyl)propane.

H. Dote, H. Yasuhara, and S. Nakashima,

V Summary of chapter V

We obtained several types of crystals in mixed crystals and successfully analyzed the structures of light-blue crystals and blue crystals. Firstly ionic crystals ($[H_2(bpp)][Zn(NCS)_4]$) appeared. The structure is built up as spiral. And then, neutral 1D chain formed by releasing HNCS from the cation and anion. This change could be pursued by using mixed crystals, because such change appears with the color change.

Chapter VI

Anion-mixed complexes with 1,3-bis(4-pyridyl)propane[1]

[1] Crystal structure and spin state of mixed crystals of iron with NCS and $NCBH_3$ for the assembled complexes bridged by 1,3-bis(4-pyridyl)propanes.

H. Dote, H. Yasuhara, and S. Nakashima, *Journal of Radioanalytical and Nuclear Chemistry*, **2015**, 303, *2*, pp 1589-1593.

VI Summary of chapter VI

We tried to synthesize anion-mixed complexes. For the results of elemental analysis, fraction of NCS is slightly more than preparation fraction for both enclathrating complexes and no-clathrated complexes. Powder X-ray diffraction shows the peak top of the spectra shifts higher degree in proportion to the fraction of NCS. The results suit with the results in single crystal X-ray analysis. Although Mössbauer spectra show the comparison of the fraction of $Fe(NCS)_2$ unit deduced from the area fraction of Mössbauer spectra with that obtained from elemental analyses and the fraction of low spin state in the $Fe(NCBH_3)_2$ unit changed with the change of X, Mössbauer spectra can also be analyzed that the samples consist only $Fe(NCS)_2$ and $Fe(NCBH_3)_2$ unit, not $Fe(NCS)(NCBH_3)$ unit.

Chapter VII

Anion-mixed complexes with 1,2-bis(4-pyridyl)ethane[1]

[1]Ligand Field of Fe(NCS)($NCBH_3$) Unit for the Assembled Complexes Bridged by 1,2-bis(4-pyridyl)ethane.

H. Dote, M. Kaneko, K. Inoue, and S. Nakashima

VII-4 Summary of chapter VII

Elemental analysis shows that the fractions of NCS are more than the preparation fraction. The structure of complex **1** and **3** are similar to structure of $Fe(NCS)_2$ complex but complex **3** has slightly short Fe-N length at 78 K because the sample likely includes a part of $Fe(NCS)(NCBH_3)$ unit becoming LS state at 78 K. DFT calculation shows ligand field strength of $Fe(NCS)(NCBH_3)$ unit is between that of $Fe(NCS)_2$ and $Fe(NCBH_3)_2$ complex. Mössbauer spectroscopy shows that complexes without guest molecules have $Fe(NCS)(NCBH_3)$ unit and either $Fe(NCS)_2$ unit or $Fe(NCBH_3)_2$ unit. SQUID measurement shows that the samples enclathrating *p*-DCB have stepwise spin transition, and SQUID measurement and DFT calculation estimated that the sample has $Fe(NCS)_2$ unit and $Fe(NCS)(NCBH_3)$ unit. The stepwise transition was simulated by using the result of elemental analysis. This SCO is rare case by mixing anion to control the ligand field. UV spectra show that *d-d* transition energy becomes higher in the order of $Fe(NCS)_2$, $Fe(NCS)(NCBH_3)$, and $Fe(NCBH_3)_2$ complex. The sample showing SCO has propeller type dihedral angle of pyridine-anion and the angle is nearly half of pyridine-pyridine.

Chapter VIII

General Conclusion

VIII General Conclusion

We obtained several types of crystals in mixed crystals. In studies of two metals-mixed complexes, the structure, Mössbauer spectra, and characteristics of the complexes are similar to pure iron complexes when using the same anion. In the study, notably difference which is in $NCBH_3$ complex for mixed manganese complex having more HS than pure iron complex was shown. This is depending on chemical pressure caused by diluted iron by manganese which has larger ionic radius. No iron complexes whose central metals are zinc and cobalt were also synthesized. The complexes have two types of color, red and blue, appeared. The structure of red crystals is similar to pure iron complexes, which is 2D inter-penetrated structure and that of blue crystals is similar to pure zinc complexes, which is 1D chain.

While in studies of three metals mixed complexes, we successfully analyzed the structures of light-blue crystals and presumed the structures of blue crystals. Firstly ionic crystals ($[H_2(bpp)][Zn(NCS)_4]$) appeared. And then, neutral 1D chain formed by releasing HNCS from the cation and anion. This change could be pursued by using mixed crystals, because such change appears with the color change. This shows $[H_2(bpp)][Zn(NCS)_4]$ is kinetics product and $Zn(NCS)_2(bpp)$ is thermodynamics product.

Anion-mixed complexes were synthesized in several conditions by using NCS, $NCBH_3$, and bpp or bpa. For bpp complexes, all the spectra consist of $Fe(NCS)_2$ unit and $Fe(NCBH_3)_2$ unit, and we don't have to take $Fe(NCS)(NCBH_3)$ unit into consideration for the analysis of the spectra. That is to say, they consist $Fe(NCS)_2$ and $Fe(NCBH_3)_2$ complexes randomly. However LS in $Fe(NCBH_3)_2$ unit is decreased when fraction of NCS is from 0 to around 1.4 and increased when fraction of NCS is from around 1.4 to 2. This is depending on effect of mixed anion.

For bpa complexes, Mössbauer spectra show different spectra which have smaller ΔEq than pure complexes, and the quadrupole splitting value is not changed by

increasing or decreasing fraction of NCS. Therefore we assumed $Fe(NCS)(NCBH_3)$ units exist. However the spectra are temperature-independent HS state. Thus to obtain complexes showing SCO phenomenon and having asymmetric unit, we synthesized enclathrating *p*-DCB complexes. Mössbauer spectroscopy shows that the complexes show SCO phenomenon. SQUID measurement and DFT calculation show transition temperature for $Fe(NCS)(NCBH_3)$ unit is between that for $Fe(NCS)_2$ unit and $Fe(NCBH_3)_2$ unit. That is to say, we successfully control the ligand field and transition temperature.